# Sensitive on-chip methane detection with a cryptophane-A cladded Mach-Zehnder interferometer

**Firehun Tsige Dullo,[1,2] Susan Lindecrantz,[1] Jana Jágerská,[1,*] Jørn H. Hansen,[3] Magnus Engqvist,[3] Stian Andre Solbø,[2] and Olav Gaute Hellesø[1]**

[1]*Department of Physics and Technology, UiT The Arctic University of Norway, 9037 Tromsø, Norway*

[2]*Northern Research Institute, 9294 Tromsø, Norway*

[3]*Department of Chemistry, UiT The Arctic University of Norway, 9037 Tromsø, Norway*

[*]*jana.jagerska@uit.no*

**Abstract:** We report a methane sensor based on an integrated Mach-Zehnder interferometer, which is cladded by a styrene-acrylonitrile film incorporating cryptophane-A. Cryptophane-A is a supramolecular compound able to selectively trap methane, and its presence in the cladding leads to a 17-fold sensitivity enhancement. Our approach, based on 3 cm-long low-loss $Si_3N_4$ rib waveguides, results in a detection limit as low as 17 ppm. This is 1-2 orders of magnitude lower than typically achieved with chip-scale low-cost sensors.

© 2015 Optical Society of America

**OCIS codes:** (130.3120) Integrated optics devices; (130.6010) Sensors; (230.3120) Integrated optics devices.

## References and links

1. IPCC Fifth Assessment Report (WGI AR5), *Climate Change 2013: The Physical Science Basis, Summary for Policymakers* (Cambridge University, 2013).
2. J. Hodgkinson and R. P. Tatam, "Optical gas sensing: a review," Meas. Sci. Technol. **24**, 012004 (2013).
3. J. Shemshada, S. M. Aminossadati, M. S. Kizil, "A review of developments in near infrared methane detection based on tunable diode laser," Sens. Actuators B Chem. **171-172**, 77–92 (2012).
4. N. S. Lawrence, "Analytical detection methodologies for methane and related hydrocarbons," Talanta **69**, 385–392 (2006).
5. T. Brotin and J.-P. Dutasta, "Cryptophanes and Their Complexes–Present and Future," Chem. Rev. **109**, 88–130 (2009).
6. L. Garel, J.-P. Dutasta, and A. Collet, "Complexation of Methane and Chlorofluorocarbons by Cryptophane–A in Organic Solution," Angew. Chem. Int. Ed. Engl. **32**, 1169–1171, (1993).
7. E. Souteyrand, D. Nicolas, J.R. Martin, J.P. Chauvet, H. Perez, "Behaviour of cryptophane molecules in gas media," Sens. Actuators B Chem. **33**, 182–187 (1996).
8. K. E. Chaffee, H. A. Fogarty, T. Brotin, B. M. Goodson, and J.-P. Dutasta. "Encapsulation of small gas molecules by cryptophane–111 in organic solution. 1. Size-and shape-selective complexation of simple hydrocarbons," J. Phys. Chem. A **113**, 13675–13684 (2009).
9. M. Benounis, N. Jaffrezic-Renault, J.-P. Dutasta, K. Cherif, and A. Abdelghani, "Study of a new evanescent wave optical fibre sensor for methane detection based on cryptophane molecules," Sens. Actuators B Chem. **107**, 32–39 (2005).
10. J. Yang, Ch. Tao, X. Li, G. Zhu, and W. Chen, "Long-period fiber grating sensor with a styrene-acrylonitrile nano-film incorporating cryptophane A for methane detection," Opt. Express **19**, 14696–14706 (2011).
11. J. Yang, L. Zhou, J. Huang, Ch. Tao, X. Li, and W. Chen, "Sensitivity enhancing of transition mode long-period fiber grating as methane sensor using high refractive index polycarbonate/cryptophane A overlay deposition," Sens. Actuators B Chem. **207**, 477–480 (2015)

#245563 Received 10 Jul 2015; revised 21 Sep 2015; accepted 23 Oct 2015; published 24 Nov 2015
© 2015 OSA

12. C. Boulart, M. C. Mowlem, D. P. Connelly, J.-P. Dutasta, and Ch. R. German, "A novel, low-cost, high performance dissolved methane sensor for aqueous environments," Opt. Express **16**, 12607–12617 (2008) .
13. C. Wagner, C., J. Frankenberger, and Peter P. Deimel. "Optical pressure sensor based on a Mach-Zehnder interferometer integrated with a lateral a-Si: H pin photodiode," IEEE Photon. Tech. Lett. **5**, 1257–1259 (1993).
14. N. Fabricius, G. Gauglitz, and J. Ingenhoff, "A gas sensor based on an integrated optical Mach-Zehnder interferometer," Sens. Actuators B Chem. **7**, 672–676, (1992).
15. A. L. Siarkowski, L. F. Hernandez, B.-H. Viana Borges, N. I.Morimoto, "Sensing based on Mach-Zehnder interferometer and hydrophobic thin films used on volatile organic compounds detection," Opt. Eng. **51**, 054401 (2012).
16. A. Densmore, D. X. Xu, S. Janz, P. Waldron, J. Lapointe, T. Mischki, G. Lopinski, A. Delâge, J. H. Schmid, and P. Cheben, "Sensitive label-free biomolecular detection using thin silicon waveguides," Adv. Opt. Technol. **2008**, 725967 (2008).
17. P. Kozma, F. Kehl, E. Ehrentreich-Frster, Ch. Stamm, F. F. Bier, "Integrated planar optical waveguide interferometer biosensors: A comparative review," Biosens. Bioelectron. **58**, 287–307, (2014).
18. F. Prieto, B. Sepúlveda, A. Calle, A. Llobera, C. Dominguez, A. Abad, and A. Montoya, "An integrated optical interferometric nanodevice based on silicon technology for biosensor applications," Nanotechnology **14**, 907–912 (2003).
19. S. Lindecrantz, J.-C. Tinguely, B. S. Ahluwalia, O. G. Hellesø, "Characterization of a waveguide Mach-Zehnder interferometer using PDMS as a cover layer," J. Eur. Opt. Soc, Rapid Publ. **10**,1990–2573 (2015).
20. F. T. Dullo, J.-C. Tinguely, S. A. Solbø, and O. G. Hellesø, "Single-mode limit and bending losses for shallow rib $Si_3N_4$ waveguides," IEEE Photon. J. **7**, 1–11 (2015).
21. J. Canceill, and A. Collet, "Two-step synthesis of D 3 and C 3h cryptophanes," J. Chem. Soc., Chem. Commun. **9**, 582–584 (1988).
22. N. Aissaoui, L. Bergaoui, J. Landoulsi, J.-F. Lambert, and S. Boujday, "Silane Layers on Silicon Surfaces: Mechanism of Interaction, Stability, and Influence on Protein Adsorption," Langmuir **28**, 656–665 (2012).
23. D. MacDougall, W. B. Crummett, "Guidelines for data acquisition and data quality evaluation in environmental chemistry," Anal. Chem. **52**, 2242–2249 (1980).
24. H.-P. Loock, P. D. Wentzell, "Detection limits of chemical sensors: Applications and misapplications," Sens. Actuators B Chem. **173**, 157–163 (2012).
25. D. R. Jacobson, N. S. Khan, R. Coll, R. Fitzgerald, L. Laureano-Prez, Y. Bai and I. J. Dmochowskia, "Measurement of radon and xenon binding to a cryptophane molecular host," Proc Natl. Acad. Sci. U.S.A. **108**, 10969–10973 (2011).
26. Z. Takacs, E. Steiner, J. Kowalewski, and T. Brotin, "NMR Investigation of Chloromethane Complexes of Cryptophane-A and Its Analogue with Butoxy Groups," J. Phys. Chem. B **118**, 2134–2146 (2014).

## 1. Introduction

Interest in methane detection has increased in recent years due to focus on the environmental effects of the greenhouse gases and climate change. Methane ($CH_4$) has approximately 30 times higher global warming potential than $CO_2$ and its amount in the atmosphere has increased by a factor of 2.5 since pre-industrial times: from 0.7 ppm to the current 1.8 ppm [1]. In order to better understand the global methane cycle, it is essential to quantify the atmospheric methane sources, including emissions from remote and inaccessible wetlands, permafrost and methane clathrates. Such a task requires the availability of low-cost and sensitive methane sensors, which are sufficiently small to be carried by lightweight planes or drones, and at the same time robust enough to be operated in extreme weather conditions. The currently available sensors are traditionally limited to high-end laboratory equipment, such as gas chromatographs, mass spectrometers or near-infrared and mid-infrared laser spectrometers, which perform extremely well in terms of sensitivity (ppt levels), specificity (interference-free) and long term stability, but are bulky and expensive [2, 3]. On the other hand, there are ultra low-cost devices such as nondispersive infrared sensors, pellistors, metal-oxide or electrochemical gas sensors, but these suffer from limited sensitivity, long-term drift and cross-responsivity to other chemical species [4].

An alternative approach to methane detection is based on cryptophanes [5], which are supramolecular compounds that form a host cavity. The cavity can selectively capture molecules whose dimensions are compatible with the cavity size. Cryptophane-A, the smallest of the series, exhibits a strong affinity towards methane [6–8]. When incorporated into polymer

#245563 Received 10 Jul 2015; revised 21 Sep 2015; accepted 23 Oct 2015; published 24 Nov 2015
© 2015 OSA

solutions such as Polydimethylsiloxane (PDMS) or Styrene-Acrylonitrile (SAN), the resulting transparent films can be used as a sensitive cladding layer for optical refractive index sensors. An optical fibre sensor for methane detection based on cryptophane molecules incorporated in a PDMS cladding was first reported in 2005 by Bernouis et al. [9]. Since then, several different sensor designs were proposed. Long-period fiber grating sensors with a SAN and polycarbonate overlay [10, 11] have achieved a detection limit down to 0.1 vol. %. Another design, a surface plasmon resonance sensor for methane detection in water [12], has reached a remarkably low detection limit of 0.2 nM, which shows the potential of cryptophane-based sensing for specific methane detection down to ambient $CH_4$ concentrations. Nevertheless, the reported techniques unanimously rely on the measurement of resonance shifts, which implies the use of a tuneable laser source or a spectrometer. This increases the sensor price as well as its footprint.

On-chip interferometric techniques represent a solution to overcome this drawback. In particular, the waveguide Mach-Zehnder interferometer is highly appealing as it is sensitive to very small refractive index variations. It has been successfully employed for a wide range of applications, such as sensing of pressure [13], gases [14], volatile organic compounds [15], DNA/RNA, proteins and other biological molecules [16, 17]. Several sensors, including a reference Mach-Zehnder interferometer, can be combined on a single chip [17], resulting in a compact and stable device. The sensitivity range of Mach-Zehnder interferometers can be adapted to the application by choosing the waveguide length, and since they do not require a tuneable laser, they can be produced at a competitive price.

In this work, we adopt the above strategy to develop an on-chip methane sensor based on a Mach-Zehnder interferometer. The device is sensitised to methane by incorporating cryptophane-A molecules in the waveguide cladding, which results in more than one order of magnitude sensitivity and selectivity enhancement and a detection limit down to ppm levels. As such, it is an excellent candidate for quantification of methane release from a multitude of natural and anthropogenic emission sources.

## 2. Sensor design and principle of operation

Figure 1 shows an integrated Mach-Zehnder interferometer, where the optical signal is split into two branches: a reference arm which is protected from the surrounding environment and a sensing arm which is exposed to the analyte. The presence of the analyte modifies the refractive index in the sensing arm, resulting in a phase difference relative to the reference arm. This phase difference is recovered after the two arms are recombined into a single output, resulting in an interference signal:

$$I_T = I_S + I_R + 2\sqrt{I_S I_R}\cos(\Delta\phi_S + \Delta\phi_0) \tag{1}$$

Here $I_S$ and $I_R$ are the intensities of the light propagating in the sensing and the reference arm, respectively, $\Delta\phi_0$ is the initial phase difference due to unmatched optical lengths of the two arms, and $\Delta\phi_S$ is the phase difference induced by the analyte.

### *2.1. Waveguide design*

The sensor is based on silicon nitride ($Si_3N_4$) shallow rib waveguides on a silica buffer layer, fabricated by low-pressure vapour deposition and reactive-ion etching as detailed in [18, 19]. The chosen material combination exhibits good transparency in both the visible and the near-infrared range and provides for high refractive index contrast and strong lateral confinement of the optical field. Also as schematically depicted in Fig. 1, the Mach-Zehnder interferometer is top-cladded with a 1 μm-thick silica layer, with a 25 μm-wide sensing window opened above the sensing arm. Devices were fabricated with sensing lengths of 1, 2 and 3 cm.

Figure 2 shows the cross-sectional view and an atomic force microscope (AFM) image of the waveguide, characterised by a core thickness of 150 nm, rib height of 5 nm and 2 μm in width.

#245563 Received 10 Jul 2015; revised 21 Sep 2015; accepted 23 Oct 2015; published 24 Nov 2015
© 2015 OSA

This design is a result of an optimisation step in order to achieve low propagation losses and a high mode-overlap with the top cladding material [19, 20].

Rib waveguides are superior to strip and slot waveguides in terms of propagation loss because of a small spatial overlap of the optical mode with the shallow-etched side-walls. A propagation loss of only 0.8 dB/cm was measured for the silica-cladded waveguides, while the polymer-cladded waveguides with cryptophane-A exhibited a slightly higher loss of 1.3 dB/cm.

As the condition of single-mode operation is indispensable for Mach-Zehnder interferometers, the waveguide dimensions were carefully chosen to support a single TE and a single TM mode at the operating wavelength $\lambda$ = 785 nm. The TM mode extends more into the top cladding, and therefore it is more sensitive to changes in the surrounding environment and more suitable for evanescent sensing. When covered with a polymer sensing layer (refractive index n = 1.56), it exhibits 47% overlap with the cladding as shown in Fig. 2(a).

### 2.2. *Methane-sensitive layer*

The key step for selective methane detection is the use of Cryptophane-A doped layer as a cladding on the sensing arm of the Mach-Zehnder interferometer. Cryptophane-A was prepared from commercial vanillin according to a published procedure [21] and purified by column chromatography. The synthetised material was characterised by nuclear magnetic resonance and high-resolution mass spectrometry, and found to exhibit identical properties to those reported [8] including host-guest behaviour towards methane.

Although most related publications use PDMS as the host for cryptophane-A, we opt for Styrene-acrylonitrile copolymer (SAN) that exhibits good chemical resistance and high clar-

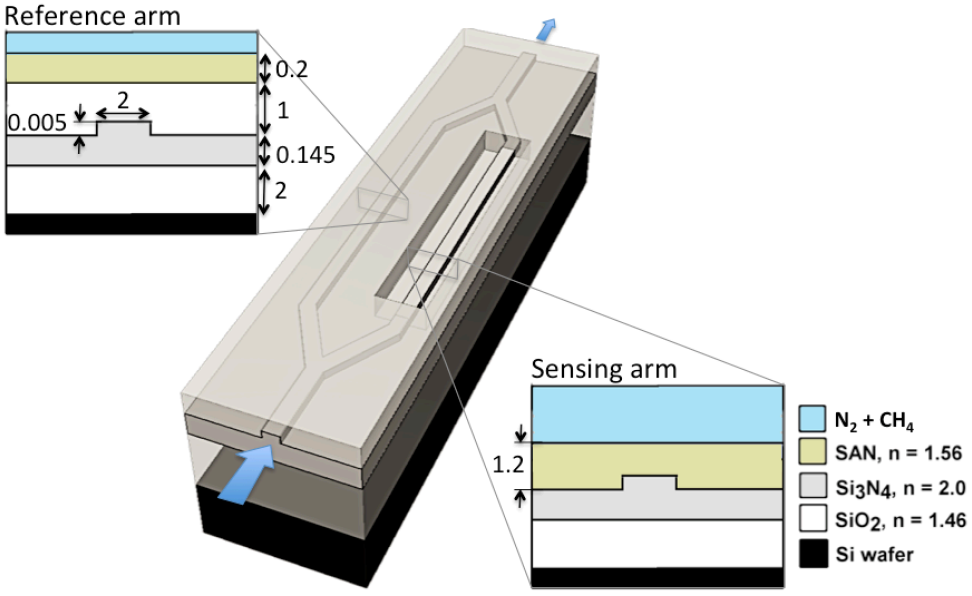


Fig. 1. 3D layout of the Mach-Zehnder interferometer, showing both the reference and the sensing arm cross-sections. The 25 µm-wide window opened above the sensing arm is filled with a cryptophane-A-doped, methane permeable polymer (SAN). This allows the methane molecules to diffuse to the waveguide surface. The waveguide dimensions and the layer thicknesses are given in micrometers.

#245563 Received 10 Jul 2015; revised 21 Sep 2015; accepted 23 Oct 2015; published 24 Nov 2015
© 2015 OSA

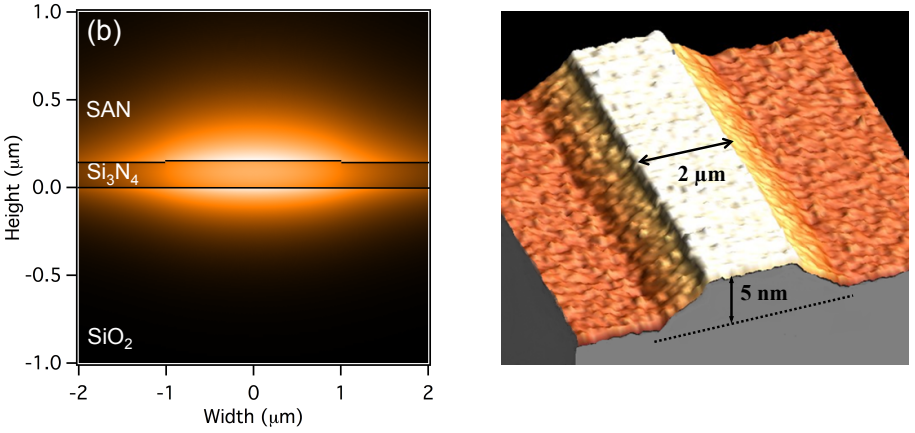


Fig. 2. The $Si_3N_4$ rib waveguide. (a) Numerically simulated mode field distribution of the fundamental TM mode over the waveguide cross-section; 47% of the optical field extends into the top polymer cladding. (b) AFM image of the waveguide surface; note the difference in the scaling of the lateral and the vertical axes.

ity. SAN was chosen for its compatibility with the solvent 1,1,2,2-tetrachloroethane, which can dissolve cryptophane much better than the solvents typically used with PDMS (e.g. tetrahydrofuran). This results in a higher transparency of the cladding film, which allows us to realise low-loss (1.3 dB/cm), centimeter-scale waveguides. Moreover, SAN has a higher refractive index (n = 1.56) than PDMS (n = 1.42), which has a positive effect on the field overlap and, thus, the sensitivity of the device.

The polymer was prepared from 5 mg (sensor A) or 1.6 mg (sensor B) of cryptophane-A solid powder and 45 mg SAN dissolved in 0.9 mL of 1,1,2,2-tetrachloroethane. Prior to deposition, the sample was silanized in 1% 3-aminopropyl-triethoxy silane (APTES)/ethanol solution in order to improve the adhesion of the polymer to the waveguide surface [22]. The cryptophane-A doped polymer was deposited on the chip surface by spin-coating at 4500 rpm for 2 minutes. As confirmed using KLA-Tencor P-6 stylus profiler, this resulted in a SAN film thickness of about 200 nm on the silica coated surface and 1200 nm inside the sensing windows (Fig. 2).

## 3. Experimental setup

The processed sensor chips were investigated using a setup that combines an optical path with a microfluidic gas-flow system for precise control of the methane flow rate and its concentration (Fig. 3). The sensor is enclosed in a microfluidic chamber with a sample volume of 0.2 mL, and mounted on a temperature-stabilised stage equipped with a Peltier element. The latter is used to control the sample temperature with an accuracy of 1 mK, and thus reduce the phase drift due to external temperature variations. TM-polarized light from a solid-state laser source emitting at 785 nm (DL785-120-SO, CrystaLaser, USA) is coupled into a polished waveguide facet using an objective lens. After propagating through the Mach-Zehnder interferometer, the output is collected at the rear sample facet by a second microscope objective and refocused on an iris, which acts as a spatial filter blocking spurious light from the sample substrate and the neighbouring slab waveguides. The output signal is detected using a silicon photodiode (NEP = $2.10^{-13}$, 20 Hz bandwidth, SM1PD1A, Thorlabs, USA) and acquired at a rate of 2 Hz with a custom-written Labview program that also monitors the temperature and regulates the gas flow.

In order to investigate the response of the device to methane, two mass-flow controllers

#245563 Received 10 Jul 2015; revised 21 Sep 2015; accepted 23 Oct 2015; published 24 Nov 2015
© 2015 OSA

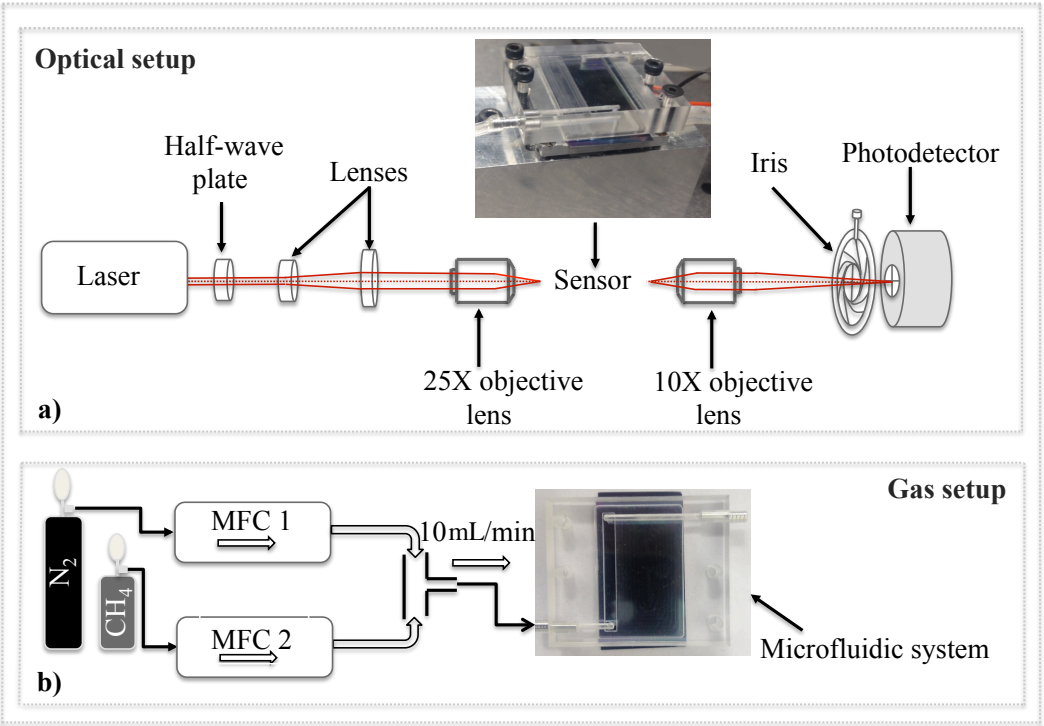


Fig. 3. Schematic diagram of (a) the optical setup and (b) the gas flow system. The top photograph shows the 25 mm × 40 mm sensor chip enclosed in a microfluidic chamber and mounted on a thermo-electrically stabilised stage.

(MFCs, 100 mL/min, EL-Flow, Bronkhorst) are used to prepare a mixture of methane and pure nitrogen (2% $CH_4$ in $N_2$). By adjusting the mixing ratios of the two gases, the methane concentration can be varied between 0 and 2%. The total gas flow through the microfluidic system is kept constant at 10 mL/min.

## 4. Results and discussion

Figure 4 shows the response of sensor A when alternately exposed to 2% methane or pure nitrogen. The intensity measured at the sensor output (Fig. 4(a)) exhibits a distinct and reproducible change each time the methane gas is introduced. According to Eq. (1), this intensity change is directly related to the phase difference between the interferometer arms, and can be expressed as:

$$\Delta\phi_S(t) = \Delta\phi_0 + \arccos\frac{I_T(t) - I_S - I_R}{2\sqrt{I_S I_R}} \tag{2}$$

Experimental values of $I_S$ and $I_R$ are obtained from the maxima and the minima of the measured intensity modulation as $I_S + I_R = (I_{max} + I_{min})/2$ and $2\sqrt{I_S}\sqrt{I_R} = (I_{max} - I_{min})/2$. The initial phase shift $\Delta\phi_0$ between the respective interferometer arms, which is always present due to different optical, thermo-optical and opto-mechanical properties, can be modified by e.g. tuning the temperature of the sensor chip. It is generally beneficial to set $\Delta\phi_0$ to $\pi/2$, i.e. in the middle of an interference fringe, where the intensity change induced by an infinitesimal phase change is maximum and thus the sensitivity of the sensor is the highest. If the phase change $\Delta\phi_S$ should exceed $\pi/2$, the result of Eq. (2) has to be unwrapped by respecting the condition of continuity of the $\Delta\phi_S(t)$ function and its first order derivative as demonstrated in Figs. 4(c) and 4(d).

#245563 Received 10 Jul 2015; revised 21 Sep 2015; accepted 23 Oct 2015; published 24 Nov 2015
© 2015 OSA

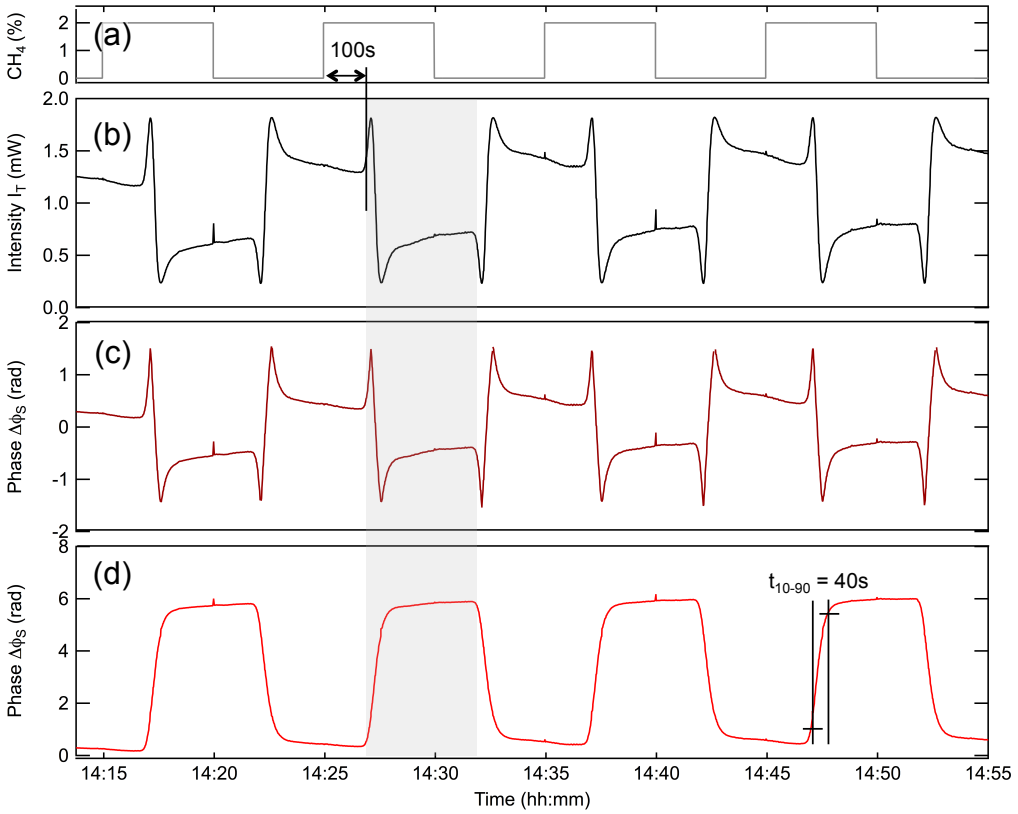


Fig. 4. Varying input methane concentration (a) and the resulting optical transmission change using sensor A (b). The corresponding phase change calculated using Eq. (2) before (c) and after unwrapping (d). The temporal offset of 100 s between the change in methane concentration and the phase response, as well as the 10% to 90% rise time of 40 s, are primarily related to the gas transport from the MFCs to the microfluidic chip. The spikes visible in the data are due to a shock wave generated upon switching between the respective MFCs.

### *4.1. Time response*

From the temporal behaviour of the phase change (Fig. 4(d)), the sensor time response, stability and repeatability can be found. After penetration of methane into the microfluidic chamber, the phase $\Delta\phi_S$ exhibits a rapid increase with a 10% to 90% rise time $t_{10-90} = 40$ s, before it stabilises within another 80 s of measurement. The measured time constant $t_{10-90}$ gives only an upper estimate of the response time, as in the current configuration it is not possible to decouple the response time of the sensor from the settling time of the MFCs upon switching (several seconds) and potential mixing of the gases prior to contact with the sensor surface.

Following the 120 s period of stabilisation, a small linear phase drift can still be observed in the measured signal. This is due to a rather high temperature sensitivity of the interferometer ($5.6\,\mathrm{rad}/^{\circ}C$) that reacts to any temperature variations of the sampled gas and the surrounding environment. The drift is expected to diminish in a system with only one flow control element. Furthermore, environmental changes of pressure and temperature can be compensated using a balanced interferometer, or by a reference sensor of identical design but no cryptophane-A contained in the polymer cladding.

#245563 Received 10 Jul 2015; revised 21 Sep 2015; accepted 23 Oct 2015; published 24 Nov 2015
© 2015 OSA

### 4.2. *Sensitivity and detection limit*

In order to experimentally investigate the sensitivity, the methane concentration was varied between 300 ppm and 2%, and the methane-induced phase change was recorded as shown for sensor A in Fig. 5(a). Despite the slow temperature drift, the reproducibility of the phase change in response to the same concentration of methane was high: if the amplitude of the phase change was taken systematically after 120 s from the rise onset, the scatter of the measured data exhibited a standard deviation of only 1%, which is a good estimate of the sensor accuracy.

Figure 5(b) shows the amplitude of the phase change plotted against the methane concentration for two sensor chips A and B that differ in the Cryptophane-A amount in the polymer cladding. Both plots exhibit a linear dependence of the phase change on the methane concentration $c$, which allows us to define the device sensitivity as:

$$S = \frac{\Delta\phi_S}{c} \tag{3}$$

Figure 5(b) also demonstrates that the amount of Cryptophane-A has a strong influence on the device sensitivity: while the sensitivity of sensor A reaches $2.67\times10^{-4}$ rad/ppm, the sensitivity of sensor B that contains about 3-times less Cryptophane-A is roughly 3-times lower.

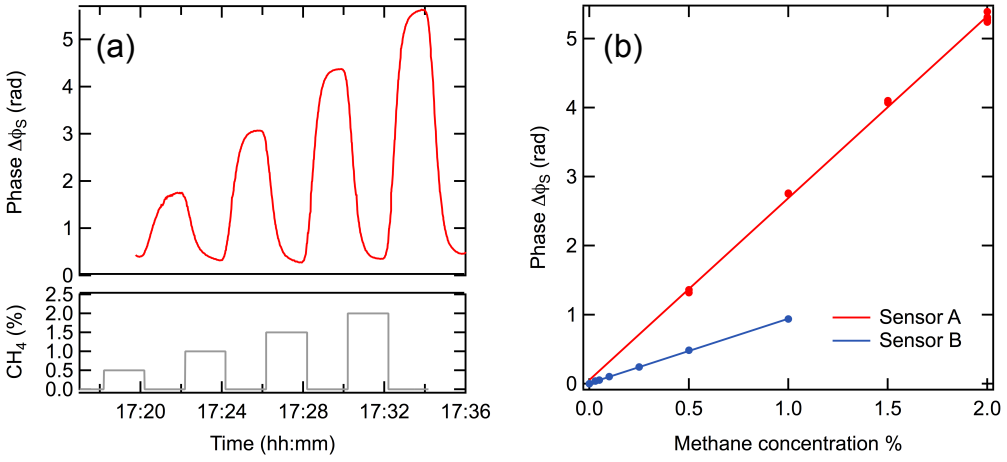


Fig. 5. (a) Recorded phase change $\Delta\phi_S$ for sensor A and 4 different methane concentrations. (b) Phase change versus methane concentration for sensors A (red) and B (blue).

The limit of detection (LOD, 99% confidence level) was calculated according to the procedure suggested by the American Chemical Society [23, 24]:

$$LOD = \frac{2.821\sigma_y}{S}, \tag{4}$$

where $S$ is the sensitivity and $\sigma_y$ is the standard deviation of the measurement at a concentration close to the expected detection limit. To find $\sigma_y$, the methane concentration was cycled 10 times between 0 and 300 ppm, and the read-out was averaged during the last 15 s of each cycle. This procedure resulted in $\sigma_y = 1.65 \times 10^{-3}$, which translates into a detection limit of 17 ppm for sensor A and 50 ppm for sensor B. These values are significantly lower than typically achieved with low-cost calorimetric or solid state sensors [4], manifesting the potential of our on-chip sensor for practical applications. The actual sensitivities and the related detection limits are summarized for both sensors in Table 1.

#245563 Received 10 Jul 2015; revised 21 Sep 2015; accepted 23 Oct 2015; published 24 Nov 2015
© 2015 OSA

Table 1. Sensitivity and limit of detection for the measured sensors.

| Sensor | Crypt.-A : SAN | Sensitivity ($10^{-4}$ rad/ppm) | $\sigma_y$ ($10^{-3}$ rad) | LOD (ppm) |
|---|---|---|---|---|
| Sensor A | 1:9 | 2.67 | 1.65 | 17 |
| Sensor B | 1:28 | 0.94 | 1.65 | 50 |

### *4.3. Sensitivity enhancement due to cryptophane*

To evaluate the sensitivity enhancement due to cryptophane, we compared the above results to the response of a refractive index sensor based on the same Mach-Zehnder interferometer, but with no cryptophane-A in the polymer cladding. As shown in Fig. 6, the phase change of a 3 cm long sensor without Cryptophane-A is 0.31 rad. On the other hand, sensor A exhibits, for the same methane concentration, a phase change of 5.28 rad. This demonstrates a 17-fold sensitivity enhancement, which is likely to further increase with the amount of Cryptophane-A. However, a detailed study relating the concentration of the cryptophane to the sensitivity enhancement, scattering loss of the waveguide and the limit of detection, is still needed in order to explore the full potential of the current approach.

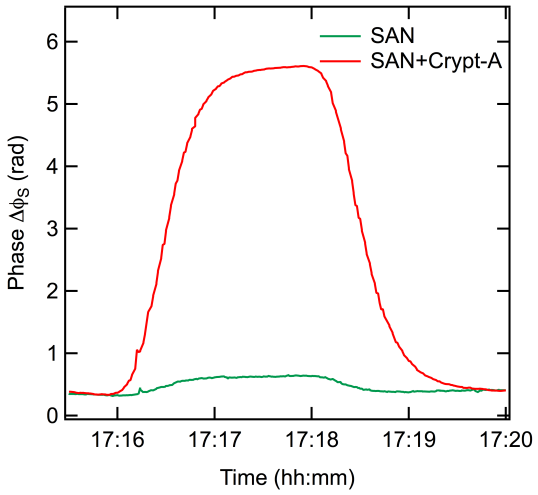


Fig. 6. Comparison of the phase response to 2% methane from sensors with and without cryptophane-A, showing a 17-fold sensitivity enhancement due to cryptophane.

### *4.4. Cross-sensitivity*

The sensitivity enhancement observed for the cryptophane-cladded sensors indicates that 16/17 of the total phase change is related to the methane encapsulation in the cryptophane cages. Only the remaining fraction of the phase change is non-specific, i.e., related to the refractive index change of the gas regardless of its chemical composition. Therefore, the cross-sensitivity of the sensor to other gases is scaled by the same factor, and can be eliminated by using a reference sensor cladded by a pure SAN film without the cryptophane component. Nevertheless, interference with the few species that also exhibit high affinity to cryptophane-A, such as xenon, radon and chloromethanes [8, 25, 26], is hard to avoid. This should be quantified and taken into consideration when targeting practical applications.

#245563 Received 10 Jul 2015; revised 21 Sep 2015; accepted 23 Oct 2015; published 24 Nov 2015
© 2015 OSA

## 5. Conclusions

In summary, we have demonstrated an on-chip methane sensor based on an integrated Mach-Zehnder interferometer, which uses a polymer cladding doped with cryptophane-A to increase the sensitivity and selectivity. The choice of styrene-acrylonitrile as a host polymer for cryptophane molecules was a key to the successful realisation of low-loss centimetre-scale waveguides, constituting the principal building block of the sensor. Our approach resulted in a 17-fold sensitivity enhancement compared to a refractive index sensor, and a detection limit as low as 17 ppm. This sensitivity is sufficient for practical use in safety and process control, as well as in some environmental applications such as monitoring of methane emission sources. Furthermore, the 1200 nm-thin cladding, matched to the decay length of the evanescent field, provides for fast methane diffusion and, hence, fast response of the sensor. The sensor chips are small, light, and, when pigtailed with optical fibres, sufficiently rigid for air-borne deployment. Moreover, since they are patterned with standard photolithography, the sensor chips are cheap and eligible for mass production.

In the next step, our efforts will focus on increasing the chip sensitivity by optimising the cryptophane cage size, as well as shifting the excitation wavelength to a region of strong methane dispersion. Moreover, a new chip design comprising reference interferometers will be proposed to compensate for temperature and pressure drift and to increase the long-term stability and specificity of the sensor. Our final aim is to make a prototype sensor for installation on a civilian drone, to conduct surveys of remote and poorly-accessible natural methane sources.

## Acknowledgments

The first two authors contributed equally to this work. The work is a part of the project Sensor Technology, funded by the Research Council of Norway (grant 195308). The authors want tho acknowledge the support from Laura Lechuga Gómez (ICN, Barcelona, Spain), as well as Carlos Dominguez and co-workers (CSIC, Barcelona, Spain) who fabricated the waveguides.

#245563 Received 10 Jul 2015; revised 21 Sep 2015; accepted 23 Oct 2015; published 24 Nov 2015
© 2015 OSA